DTU Library

Nanocantilever based mass sensor integrated with cmos circuitry

Davis, Zachary James; Abadal, G.; Campabadal, F.; Figueras, E.; Esteve, J.; Verd, J.; Perez-Murano, F.; Borrise, X; Nilsson, S. G.; Miximov, I.

Total number of authors:
13

Published in:
Proceedings of the 12th International Conference on Solid-State Sensors, Actuators and Microsystems (Transducers)

Publication date:
2003

Document Version
Publisher's PDF, also known as Version of record

NANOCANTILEVER BASED MASS SENSOR INTEGRATED WITH CMOS CIRCUITRY

Zachary James Davis*, Gabriel Abadal**, Esko Forsén*, Ole Hansen*, Francesca Campabadal***, Edwardo Figueras***, Jaume Esteve***, Jaume Verd**, Francesc Pérez-Murano***, Xevi Borrisé**, Sara G. Nilsson****, Ivan Maximov****, Lars Montelius****, Núria Barniol** and Anja Boisen*

Mikroelektronik Centret, Denmark Technical University, 2800 Lyngby, Denmark*
Dept. Enginyeria Electrònica, Universitat Autònoma Barcelona, E- 08193 Bellaterra, Spain**
Institut de Microelectrònica Barcelona (IMB-CNM), Campus UAB, 08193 Bellaterra, Spain***
Solid State Physics & The Nanometer Consortium, University of Lund, Sweden****
Tel.: +45 45255733, Fax: +45 45258872, e-mail: zd@mic.dtu.dk

ABSTRACT

We have demonstrated the successful integration of a cantilever based mass detector with standard CMOS circuitry. The purpose of the circuitry is to facilitate the readout of the cantilever's deflection in order to measure resonant frequency shifts of the cantilever. The principle and design of the mass detector are presented showing that miniaturization of such cantilever based resonant devices leads to highly sensitive mass sensors, which have the potential to detect single molecules. The design of the readout circuitry used for the first electrical characterization of an integrated cantilever is described in detail. The integration of the cantilever is a post processing module and the full process sequence is discussed. One of the main challenges during the fabrication of the cantilevers is sticktion of the cantilever to the bottom substrate after underetching. Two dry release techniques were used to solve the problem, namely freeze-drying and resist-assisted release. The fabrication results of cantilevers defined by laser and E-beam lithography are shown. Finally, an AFM based characterization setup is presented and the electrical characterization of a laser-defined cantilever fully integrated with CMOS circuitry is demonstrated. The electrical characterization of the device shows that the resonant behavior of the cantilever depends on the applied voltages, which corresponds to theory.

INTRODUCTION

The growing need for faster, cheaper and more sensitive sensors is pushing the world of MEMS into the nano regime (NEMS). This paper presents the fabrication and characterization of a mass sensor, which consists of a nanometer-sized cantilever fully integrated with standard CMOS circuitry. The cantilever is electrostatically excited laterally into resonance and the cantilever's vibrational amplitude is monitored by measuring the capacitance change between the vibrating cantilever and a fixed parallel electrode using integrated CMOS circuitry. The concept of the sensor can be seen in figure 1. By monitoring the change in the cantilever's resonant frequency, a mass change of the cantilever can be measured. The minimum detectable mass change of the sensor can be approximated by the simple formula [1]:

$$\delta m \cong 0.209 \frac{k}{f_0^3} \delta f \qquad (1)$$

where k is the spring constant and f_0 is the resonant frequency of the cantilever. By scaling down the dimensions of the cantilever the resonant frequency increases while the spring constant can be held constant. Thus, miniaturization of the device leads to an increase in mass sensitivity. Compared to other groups [2,3] this device is very compact, due to the integrated readout, and well suited for both vacuum and gas measurements.

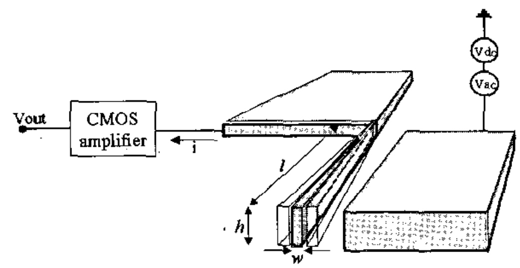

Figure 1: Schematic illustration of the mass sensor device, which is based on a laterally vibrating cantilever with electrostatic excitation and capacitive readout.

DESIGN

The current through the device can be expressed as:

$$I = \frac{\partial}{\partial t}(CV) = C\frac{\partial V}{\partial t} + V\frac{\partial C}{\partial t} \qquad (2)$$

where the first term is the normal capacitive current through the capacitance of the system and the second term is the mechanical current induced by the vibration of the cantilever. In order to minimize the first term the parasitic capacitances in the system must be minimized, thus the need for careful integration of the cantilever device with CMOS circuitry.

The design of the device consists of the cantilever described above and the CMOS circuitry. The circuit design is based on an amplifier and a voltage follower as seen in figure 2. The amplifier is a current mirror with three NMOS and one PMOS transistors. Basically, the charge on the cantilever is connected to the gate of the first NMOS transistor. If this transistor is polarized in its linear region, the mechanical current, when the cantilever is in resonance, will fluctuate the gate charge and thus fluctuate the current flowing in the current

0-7803-7731-1/03/$17.00 ©2003 IEEE

mirror. The output of the amplifier is connected to an operational amplifier with unity gain, which gives a good impedance adaption at the output of the amplifier.

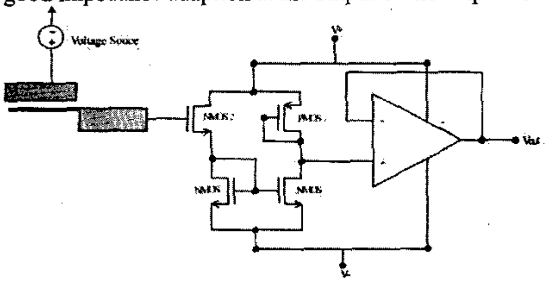

Figure 2: Circuit diagram of the amplification circuit integrated with the cantilever device.

The electrical characterization of the amplifier circuit is seen in figure 3, which has been performed prior to post processing of the CMOS. In figure 3a the output voltage versus the input voltage is presented. The linear region of the curve, around Vin=0, is the region where the circuit has a finite gain, which is approximately 6. In figure 3b the frequency response of the circuit is shown, showing that the bandwidth of the circuit is approximately 1.7MHz.

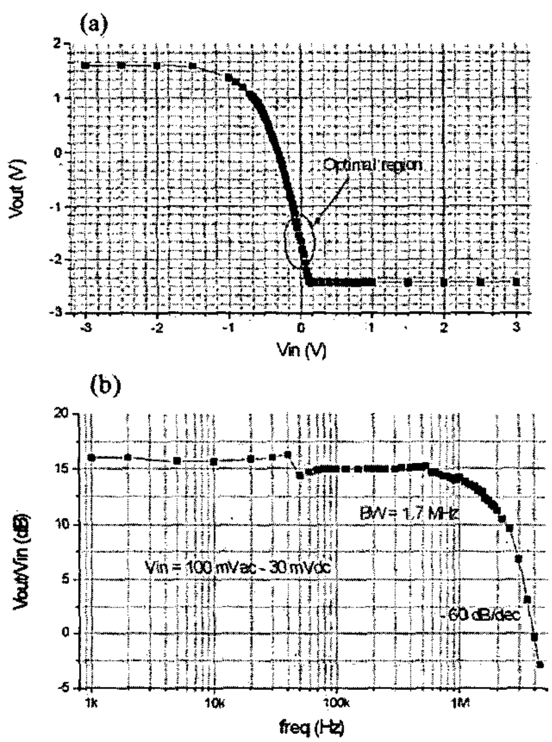

Figure 3: Characterization results of the amplification circuit described in the text. (a) The Vout versus Vin showing the linear region where the circuit has the optimal gain and (b) the frequency response of the circuit showing that the bandwidth is 1.7MHz.

In figure 4a the layout of the complete sensor device is shown, which consists of the circuit and the so-called nanoarea where the cantilever will be situated.

In figure 4b the design of the cantilever, driver electrode and comb capacitor, which is to be fabricated in the nanoarea, is shown. The function of the comb capacitor is to be able to charge the cantilever, and thus the gate of the first transistor in the amplifier circuit. The comb capacitor increases the capacitance so that the circuit can be polarized into the linear region of the output voltage, using a smaller input voltage.

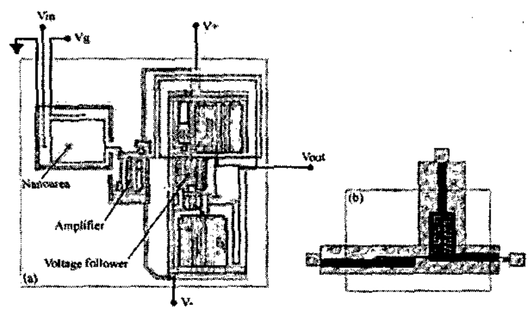

Figure 4: (a) Schematic layout of the complete mass sensor device, which consists of the nanoarea, the amplifier and the voltage follower. (b) A close-up of the nanoarea where the design of the mechanical sensor and comb capacitor is shown.

FABRICATION PROCESS

Process Sequence. The fabrication of the device is illustrated in figure 5. The realization of the cantilever is performed as a post process module on pre-fabricated CMOS chips. The CMOS technology is a standard twin well, 2-poly, 2-metal technology. The cantilever is fabricated using the bottom poly0 layer, which is highly doped. First a hole is opened in the CMOS passivation layer and the underlying poly1 layer is selectively removed by dry etching (figure 5a). Then a cantilever mask definition step is performed (Figure 5b). Three different lithography techniques are being investigated, which are laser, electron-beam and atomic force microscopy (AFM) lithography. Results on cantilever fabrication using laser lithography have been presented at Transducers '01 [3]. With electron-beam lithography (EBL) a 30nm thick Al mask is defined using lift-off technique. With AFM lithography a 10nm thick Al layer is locally oxidized with the AFM tip, and the non-oxidized Al is selectively removed in a wet chemical etch resulting in an Al oxide mask. After the mask definition, the cantilever and parallel electrode are transferred to the poly0 by dry etching (figure 5c). Finally, the structures are released in BHF, which etches the underlying 1μm thick SiO2 layer (figure 5d). Upon release of the cantilevers, drying the cantilevers from a wet state caused the cantilevers to stick to the substrate, due to capillary forces. In order to avoid these sticktion forces, two dry release techniques (freeze drying and resist-assisted release) were investigated.

Freeze-Drying. In the freeze-drying process the device is rinsed in DI water several times, directly after underetching. Then it is placed in acetone in order to remove a protective layer of resist, which is covering everything besides the nanoarea. Next, the device is rinsed in propanol and immersed in liquid tert-butanol, which has a freezing temperature of approximately 20^0C. The device is then taken from the tert-butanol and placed on a cooling plate where the tert-butanol freezes almost instantly. Subsequently, the device is placed in a vacuum chamber where the solid tert-butanol slowly evaporates to the gas phase. A disadvantage of this technique is that the tert-butanol is easily contaminated with water, thus the reproducibility of this technique is unstable.

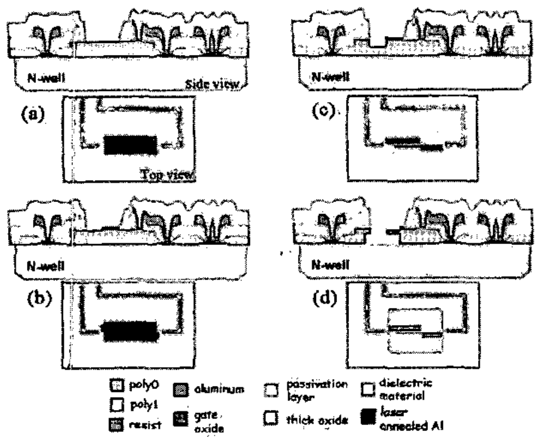

Figure 5: Fabrication process sequence of the cantilever device on CMOS circuitry.

Resist Release. In order to solve the reproducibility problems another dry release method was used. The procedure is as follows: First, the device is rinsed in DI water and immersed in acetone in order to dissolve the protective resist. Then, the device is immersed in a thin solution of resist and subsequently spun and soft baked. This treatment results in an approximately 3μm thick resist layer on top of the device, which fully encapsulates the cantilever. The resist is then etched away in an O_2 plasma. The advantages of this technique is that there are no chances of contamination and that the resist coating can act as a temporary packaging of the device, which protects the device until measurements are to be made.

Fabrication Results. In figure 6, images are shown of devices fabricated with laser lithography. With laser lithography the minimum width of the cantilever is approximately 800nm. In figure 6a, the whole device is shown just after laser lithography. In figure 6b an optical image of the nanoarea after dry etching is seen. The cantilever, driver electrode and comb capacitor are defined in the poly0 layer. Figure 6c and d show SEM images of the same nanoarea as in figure 6b. In figure 6d it is seen that the cantilever is very porous, which is due to the poor masking of the Al based mask. The Al based mask is very thin, approximately 7-10nm, and the roughness of the poly0 is much higher. Thus pinholes in the Al layer can easily occur. It is also seen that the sidewalls of the cantilever are very rough. This is probably because the laser lithography is a thermal process, where the Al is locally annealed to change the material. Since the heat dissipates both into the substrate and out into the surface, the mask is poorly defined at the edges.

In figure 7, EBL defined cantilevers are shown. In figure 7a the Al mask after lift-off is seen. In figure 7b the same device is seen after dry etching, and in figure 7c and d SEM images of a one and two electrode device are shown. Cantilevers with a width down to 300 nm have been realized by EBL, as seen in figure 7d. Also seen in figure 7d, the apex of the cantilever is slightly wider than the base of the cantilever. This is due to proximity effects while performing the EBL, and can be avoided by locally adjusting the exposure dose. The surface and sidewall roughness has improved significantly compared to the laser-defined cantilevers. The reason for this is that the Al mask is defined by lift-off technique, which is well known for producing sharply defined structures. Moreover, the thickness of the Al mask is 30nm, thus the risk of having pinholes in the mask is reduced considerably.

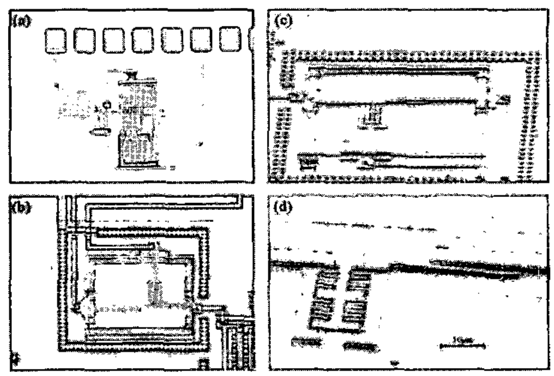

Figure 6: (a) Optical image of the complete device, (b) optical close-up image of the nanoarea with a cantilever, electrode and comb capacitor, (c) and (d) SEM images of the nanoarea.

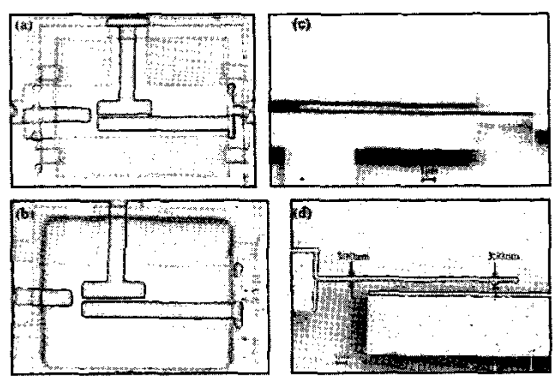

Figure 7: (a) Optical image of the EBL defined Al mask, (b) the same structure after dry etching, (c) SEM image of a two electrode device and (d) SEM image of a one electrode device.

CHARACTERIZATION

Cantilever performance. The characterization of the cantilever performance was performed in an AFM setup, where it is possible to observe the cantilever during excitation and to unstick the cantilever, if needed. The device is connected to a chip holder by wire bonding and mounted in the AFM. Figure 8(a) shows an AFM image of an EBL defined cantilever on a CMOS chip. Figure 8(b) shows an AFM image of the oscillation amplitude of a laser-defined cantilever on a CMOS chip. The image is obtained by scanning the same line across the cantilever and simultaneously sweeping the driving frequency of the AC voltage. It is seen that the oscillation amplitude is approximately 200nm at the peak resonance. Unsticktion of the cantilever can be performed by pushing the cantilever with the AFM tip and then retracting the AFM tip from the surface.

Electrical Readout. In figure 9 the readout circuitry's voltage output is shown as a function of the AC voltage frequency. The cantilevers that were measured are laser defined cantilevers with a width, height and length of 1μm, 0.6μm and 40μm respectively. The two curves correspond to two excitation voltages. The solid curve has an excitation voltage of $18V_{DC} + 7V_{ppAC}$ and the dashed curve corresponds to an excitation voltage of $20V_{DC} + 7V_{ppAC}$. It is seen that the higher excitation voltage increases the amplitude of the output signal and reduces the resonant frequency from 655kHz to 645kHz. The reason for this is that the extra DC voltage increases the electrostatic forces acting on the cantilever, which increases the vibrational amplitude and decreases the resonant frequency[1]. The quality factor (Q) of the cantilever was measured to be approximately 55. For the investigated device a mass sensitivity of approximately 10^{-16}g/Hz is expected, according to equation (1).

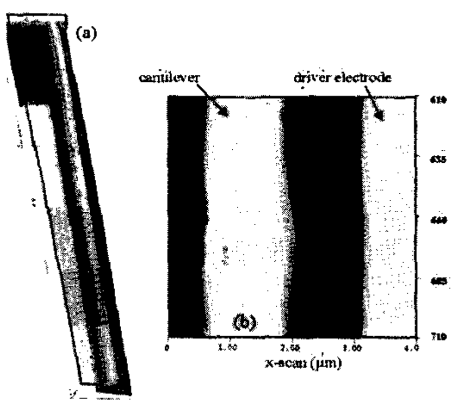

Figure 8: (a) An AFM image of an EBL defined cantilever on a CMOS circuit. (b) The resonant behaviour of a laser defined cantilever, which is measured by switching off the slow scan and varying the driving frequency while scanning the same line across the cantilever.

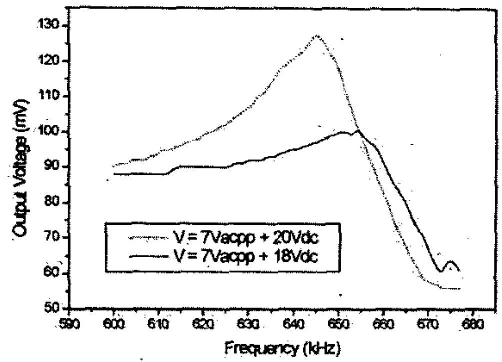

Figure 9: Electrical frequency response of a CMOS integrated cantilever device.

CONCLUSIONS AND OUTLOOK

We have demonstrated the integration of a cantilever based mass detector with CMOS circuitry. The design of the sensor is based on a laterally vibrating cantilever, which is electrostatically excited into resonance, and the mechanical current, due to the variance of the capacitance, acts as the readout. The design of the readout circuitry is based on a simple current mirror configuration and voltage follower, which has a moderate gain of approximately 6 and a high bandwidth of 1.7MHz. Laser as well as e-beam defined cantilevers have been integrated with the CMOS circuitry. EBL is seen to yield the best cantilever definition when it comes to surface and sidewall roughness as well as minimum width of the final cantilever devices. However, the laser lithography is still an interesting patterning technique for prototyping due to it high flexibility and easy and fast operation. The integrated cantilevers were characterized in an AFM set-up, where it is possible to measure the frequency response of the cantilever, without electrical readout. The frequency response has also been measured using the integrated CMOS circuit and for a laser-defined cantilever. The Q-factor was found to be approximately 55. Moreover, it was seen that by increasing the applied DC voltage the amplitude of the output signal is increased and the resonant frequency of the device is reduced.

Presently, applications of the mass sensor in vacuum and gas are being pursued.

Acknowledgments

This work is funded by an EC, Information Societies Technology (IST) Program called NANOMASS.

References

[1] Z. J. Davis, G. Abadal, B. Helbo, O. Hansen, F. Campabadal, F. Pérez-Murano, J. Esteve, E. Figueras, R. Ruiz, N. Barniol, A. Boisen, *Proceedings of Transducers 01*, pp. 72-75 (Munich 2001).
[2] A.N. Cleland and M.L. Roukes, *Appl. Phys. Lett.*, 69 (1996) 2653-2655.
[3] J. Yang, T. Ono and M. Esashi, *Sensors and Actuators*, 82 (2000) 102-107.